

Development 140, 675-686 (2013) doi:10.1242/dev.085431  
© 2013. Published by The Company of Biologists Ltd

# Functional evaluation of ES cell-derived endodermal populations reveals differences between Nodal and Activin A-guided differentiation

Alice E. Chen<sup>1,\*</sup>, Malgorzata Borowiak<sup>1,‡,§</sup>, Richard I. Sherwood<sup>1,3</sup>, Anastasie Kweudjeu<sup>1</sup> and Douglas A. Melton<sup>1,2,¶</sup>

## SUMMARY

Embryonic stem (ES) cells hold great promise with respect to their potential to be differentiated into desired cell types. Of interest are organs derived from the definitive endoderm, such as the pancreas and liver, and animal studies have revealed an essential role for Nodal in development of the definitive endoderm. Activin A is a related TGF $\beta$  member that acts through many of the same downstream signaling effectors as Nodal and is thought to mimic Nodal activity. Detailed characterization of ES cell-derived endodermal cell types by gene expression analysis *in vitro* and functional analysis *in vivo* reveal that, despite their similarity in gene expression, Nodal and Activin-derived endodermal cells exhibit a distinct difference in functional competence following transplantation into the developing mouse embryo. Pdx1-expressing cells arising from the respective endoderm populations exhibit extended differences in their competence to mature into insulin/c-peptide-expressing cells *in vivo*. Our findings underscore the importance of functional cell-type evaluation during stepwise differentiation of stem cells.

**KEY WORDS:** Definitive endoderm, Functional assay, Mouse embryo culture, Nodal, Activin

## INTRODUCTION

Directed differentiation of embryonic stem (ES) and induced pluripotent stem (iPS) cells into endodermal derivatives is intensely studied for its clinical promise in cell replacement therapies. One possible target for therapy is type 1 diabetes, a degenerative disease in which insulin-producing  $\beta$  cells of the pancreas are destroyed by autoimmune attack (Bach, 1994). The shortage of transplantable  $\beta$  cells has stimulated much interest in the *in vitro* generation of  $\beta$  cells from ES cells (Raikwar and Zavazava, 2009; Zhou and Melton, 2008). Although numerous approaches have been used to derive  $\beta$ -like cells, early attempts were lacking in efficiency, reproducibility, stringency of  $\beta$  cell identification and a thorough understanding of the origins and identities of the cell types produced (Blyszczuk et al., 2003; Hansson et al., 2004; Hori et al., 2002; Lumelsky et al., 2001; Rajagopal et al., 2003; Soria et al., 2000). This led to efforts aimed at reproducing the sequential steps that characterize normal  $\beta$  cell ontogenesis. This approach involves first coaxing ES cells into becoming definitive endoderm (DE), then providing instruction to become pancreatic in nature. Pancreatic progenitors are subsequently induced to adopt an endocrine identity, and, finally, directed towards a stable  $\beta$  cell fate. Thus, a necessary first step in the directed differentiation of ES cells towards insulin-producing  $\beta$  cells is the generation of a proper

endodermal cell population that is competent to respond to subsequent differentiation signals that specify a complete pancreatic fate.

Our understanding of endoderm formation in vertebrates stems mainly from studies in *Xenopus*, zebrafish and mouse (Lewis and Tam, 2006; Stainier, 2002; Tam et al., 2003; Tian and Meng, 2006). These studies all point to an essential *in vivo* role for Nodal, a member of the transforming growth factor beta (TGF $\beta$ ) family, in directing development of the DE (Grapin-Botton and Constam, 2007; Schier, 2003; Stainier, 2002; Zorn and Wells, 2007). Nodal signaling is activated upon interaction of Nodal ligands with activin type I and type II serine/threonine kinase receptors [ALK4 (Acvr1b), ActRIIB (Acvr2b), respectively] and the epidermal growth factor-Cripto-FRL1-Cryptic (EGF-CFC) co-receptor (Cripto; also known as Tdgf1). Stimulation of the activin receptors leads to phosphorylation and activation of the downstream transcriptional effector Smad2, which subsequently interacts with Smad4 and co-activators (e.g. Foxh1, *Xenopus* mixer) to regulate target gene expression. Activin A is a related member of the TGF $\beta$  family that initiates signaling through the same receptors as Nodal (but without Cripto), eliciting a similar cascade of intracellular events via SMADs. Activin A is therefore commonly used to mimic Nodal/Smad signaling in *in vitro* applications.

Recent work has highlighted significant progress in the differentiation of mouse and human ES cells into DE (Borowiak et al., 2009; D'Amour et al., 2005; Kubo et al., 2004; Yasunaga et al., 2005), pancreatic progenitors (Chen et al., 2009; D'Amour et al., 2006; Micallef et al., 2005) and insulin-secreting cells (Basford et al., 2012; D'Amour et al., 2006; Jiang et al., 2007; Micallef et al., 2012; Nostro et al., 2011; Rezanian et al., 2011). Furthermore, human ES cell-derived pancreatic endoderm has been shown to protect against hyperglycemia after transplantation into streptozotocin-treated mice, demonstrating the therapeutic potential of ES-derived cells (Kroon et al., 2008; Zhang et al., 2009). Despite these achievements, current protocols remain limited in efficiency

<sup>1</sup>Department of Stem Cell and Regenerative Biology, Harvard Stem Cell Institute, Harvard University, Cambridge, MA 02138, USA. <sup>2</sup>Howard Hughes Medical Institute, Harvard University, Cambridge, MA 02138, USA. <sup>3</sup>Department of Medicine and Genetics, Brigham and Women's Hospital, Harvard Medical School, Boston, MA 02115, USA.

\*Present address: Stemgent Inc., 10575 Roselle Street, San Diego, CA 92121, USA

<sup>‡</sup>Present address: Stem Cells and Regenerative Medicine Center, Baylor College of Medicine, Houston, TX 77030, USA

<sup>§</sup>These authors contributed equally to this work

<sup>¶</sup>Author for correspondence (dmelton@harvard.edu)

of  $\beta$  cell output, understanding of cell type maturity, and definition of conditions required for the complete derivation of bona fide, stable  $\beta$  cells *in vitro*. Furthermore, functional evaluation of cells at key developmental nodes during differentiation has largely been lacking. For measurable progress in the creation of pancreatic  $\beta$  cells that can be reliably used in research and therapy, we believe that stepwise validation of cell identity, including functional tests, would represent a significant advance.

We evaluated murine endoderm populations generated by treatment with recombinant Nodal and Activin proteins. We report here that, despite expressing cardinal markers of endoderm and being nearly identical at the level of global transcription, Nodal and Activin-derived mouse DE cells exhibit a striking difference in functional competence upon transplantation into the gut endoderm of the mouse embryo. Nodal- but not Activin-derived endoderm can efficiently contribute to the embryonic endoderm, differentiate into endoderm derivatives, and form primitive gut tubules upon ectopic injection. These endoderm differences impact the subsequent development of pancreatic progenitors *in vitro* as well as their competency to form clusters of insulin/c-peptide-expressing cells *in vivo*. This work advances our understanding of endodermal and pancreatic identities generated from ES cells *in vitro* and provides a grounded basis for differentiating pluripotent stem cells into functional  $\beta$  cells for disease modeling and cell therapy.

## MATERIALS AND METHODS

### Mouse ES cell culture and differentiation

Mouse ES cells (mESCs) were maintained on gelatin-coated plates with mouse embryonic fibroblasts (MEFs) in mESC medium: Dulbecco's Modified Eagle Medium (DMEM; Invitrogen), 0.1 mM non-essential amino acids (NEAA; Invitrogen), 1 $\times$  Glutamax, 1 $\times$  penicillin-streptomycin (Penn/Strep; Invitrogen), 15% fetal bovine serum (FBS; HyClone), 0.055 mM  $\beta$ -mercaptoethanol ( $\beta$ Me; Sigma) and 5 $\times$ 10<sup>5</sup> units leukemia inhibitory factor (LIF; Chemicon).

For differentiation, cultures were MEF-depleted and seeded in mESC medium at ~2700 cells/cm<sup>2</sup> on gelatin-coated dishes. Endoderm differentiation was induced the following day for 6-8 days in DMEM, 5% FBS, 0.1 mM NEAA, 1 $\times$  Glutamax, 1 $\times$  Penn/Strep, 0.055 mM  $\beta$ Me, or in advanced RPMI medium (Invitrogen), 0.2-0.5% FBS, 1 $\times$  Glutamax and 1 $\times$  Penn/Strep, with 50 ng/ml recombinant human Activin A or 1000 ng/ml recombinant mouse Nodal (R&D Systems); media changed every other day. Pancreatic differentiation was carried out as described (Borowiak et al., 2009).

### Preparation of mouse embryos for injection

CD1 males were crossed with ICR females (Charles River, Jackson Labs), with noon of the day of plug identified as embryonic day (E) 0.5. On the day before injection, E8.5 embryos were isolated from the uterus and decidua. Reichart's membrane and parietal endoderm were removed and trimmed at the base of the ectoplacental cone, leaving the yolk sac and amnion undamaged and intact to support *ex vivo* development. Embryos were cultured overnight in low-attachment 6-well dishes (Corning) in pre-warmed 50% advanced DMEM/F12 (Invitrogen), 50% heat-inactivated, sterile-filtered rat serum (Valley Biomedical) and 1 $\times$  Penn/Strep (total volume 2 ml per embryo) in a humidified incubator (5% CO<sub>2</sub>/20% O<sub>2</sub>/75% N<sub>2</sub>). The slight developmental delay provided by static culture of E8.5 mice enabled capture of E8.75-9.0 partially turned embryos, used the following morning for cell injection.

### Embryo injection and whole embryo *ex vivo* culture

Donor cells were harvested at the single-cell level and resuspended in embryo culture media at ~50,000-100,000 cells/ $\mu$ l. Resuspended cells were delivered to the primitive gut tube of E8.75 mice by injecting the anterior and posterior intestinal portals and the exposed gut lumen using pulled capillaries [50-75  $\mu$ m VWR (ID)] via mouth pipette. Following injection of ~100,000-150,000 cells, embryos were cultured in fresh embryo culture

medium for 24-30 hours in a humidified roller bottle culture unit (BTC Engineering) at 37°C (5% CO<sub>2</sub>/20% O<sub>2</sub>/75% N<sub>2</sub>).

### Flow cytometry

Differentiated cells were harvested and resuspended in PBS/5% FBS and sorted for ES-derived endoderm and pancreatic lineages by flow cytometry using FACSaria (Becton Dickinson) or MoFlo (Dako Cytomation). Following sorting, cells were centrifuged and resuspended in minimal volume for embryo or kidney capsule injection, RT-PCR or microarray analyses.

### Global gene expression analysis by microarray

Sox17-GFP(+) cells were sorted from Nodal- or Activin-treated mESC cultures. Total RNA isolated using Qiashredder and RNeasy Mini Kit (Qiagen). Biotinylated cRNA was prepared from  $\geq$ 100 ng of RNA using Illumina TotalPrep RNA Amplification Kit (Ambion) and hybridized to Illumina Mouse Genome Bead Chips (MouseRef8). Samples were prepared as biological duplicates. Data were acquired with Illumina Beadstation 500 and evaluated using BeadStudio Data Analysis Software. Full data are available in Gene Expression Omnibus (GEO) database under accession number GSE41086.

### Immunofluorescence

Cultures were fixed with fresh 4% paraformaldehyde/PBS, washed in 0.1% Triton-X in PBS (0.1% PBT) then blocked in 5% donkey serum (Jackson ImmunoResearch) in 0.1% PBT. Primary antibody was applied in 5% donkey serum in 0.1% PBT overnight at 4°C. Next day, cells were washed three times, secondary antibody was applied for 1 hour at room temperature and counterstained with DAPI (Sigma). Images captured with an Olympus IX70 microscope.

Cultured embryos were fixed with fresh 4% paraformaldehyde/PBS overnight at 4°C. Embryos were washed twice in PBS on a Nutator (TCS Scientific Corporation), equilibrated in 30% sucrose/PBS overnight, followed by equilibration in 1:1 of 30% sucrose/PBS and OCT (Tissue Tek), and then cryo-embedded in OCT. Samples were sectioned at 14  $\mu$ m onto Superfrost slides (VWR). Tissue sections were rehydrated in PBS, washed in 0.1% PBT, briefly permeabilized in 0.5% PBT then washed in 0.1% PBT. Primary and secondary antibodies were applied as described above. Slides were coverslipped using Fluoromount G (Southern Biotech).

Primary antibodies were: goat anti-SOX17 (R&D Systems), goat anti-HNF3 $\beta$ /FOXA2 (M-20), goat anti-CLDN6 (C-20), goat anti-SOX7 (E-20), rabbit anti-DAB2 (H-110), rabbit anti-SPARC (H-90), goat anti-SOX2 (Y-17) (all Santa Cruz), goat anti-PDX1 (provided by C. Wright, Vanderbilt University Medical Center, TN, USA), rabbit anti-LAM $\alpha$  (Sigma), rabbit anti-PROX1 (Covance), mouse anti-CDX2 (Biogenex), guinea pig anti-insulin (DAKO), rabbit anti-c-peptide (Linco/Millipore), rabbit anti-RFP/DsRed (MBL), chicken anti-GFP (Aves Labs), Alexa488-conjugated rabbit anti-GFP (Invitrogen). Secondary antibodies were: Alexa488- or 594-conjugated donkey anti-rabbit; Alexa488-, 594- or 647-conjugated donkey anti-goat; Alexa488-conjugated donkey anti-mouse, Alexa488-conjugated goat anti-chicken (Invitrogen), FITC-conjugated donkey anti-chicken (all Jackson Laboratories). Nuclei were visualized with DAPI (Sigma).

### Semi-quantitative and real-time quantitative PCR

For semi-quantitative PCR, total RNA from ES and differentiated cells was isolated with RNazol (Sigma). cDNA synthesis was carried out using 0.2  $\mu$ g random hexamer primer (Pharmacia Biotech), 1 $\times$  first strand reaction buffer (Invitrogen), 0.5 mM deoxyribonucleotide triphosphates (dNTPs; Denville Scientific), 0.01 mM dithiothreitol (DTT; Invitrogen), 20 units RNasin (Promega), 200 units M-MLV reverse transcriptase (Invitrogen) in 30  $\mu$ l total reaction mixture, for 1.5 hours at 37°C. Gene expression was analyzed by template cDNA PCR (25-30 cycles). PCR products were resolved on 2% agarose gels, visualized by ethidium bromide staining and images were captured via AlphaImager 3400 (Alpha Innotech). For quantitative PCR, total RNA was isolated using Trizol (Invitrogen). Reverse transcription was performed using Superscript III and PCR using SYBR Green (Invitrogen) and a MX3000p light cycler (Stratagene) ( $\leq$ 45 cycles). Expression values were normalized to  $\beta$ -actin.

### Kidney capsule injections of pancreatic progenitors

Pdx1-GFP(+) cells purified by FACS, collected in DMEM in 5% FBS, centrifuged and resuspended in minimal volume. SCID-Beige males (6–10 weeks of age) were anesthetized with Avertin (250 mg/kg; Sigma), shaved at the surgical site and cleaned with isopropanol, and iodine. The left kidney was exposed and  $0.5 \times 10^6$  cells were injected via micropipette into the upper kidney pole followed by low temperature cautery, return to original anatomical position and closure of muscle with continuous sutures and skin with wound clips. Six weeks later, transplants were recovered, fixed and processed for cryosectioning and immunostaining. Images were captured with a Zeiss LSM510 Meta confocal microscope. Quantification of C-peptide(+) cells was performed on six animals per group, 15 images per animal,  $\geq 1000$  cells counted per condition.

## RESULTS

### Nodal and Activin A promote the differentiation of highly similar definitive endoderm profiles *in vitro*

Although some reports have included brief mention of Nodal in the induction of mesendoderm (Tada et al., 2005) and endoderm (Hansson et al., 2009), current protocols for differentiating ES cells into endoderm have predominantly involved the use of Activin A (D'Amour et al., 2005; Gadue et al., 2006; Kubo et al., 2004; Yasunaga et al., 2005; Nostro et al., 2011). Nodal, however, is an essential signal during vertebrate gastrulation and specification of the DE (Ding et al., 1998; Lowe et al., 2001; Vincent et al., 2003). As Activin and Nodal signaling are similar, but not identical, we compared the capacity of Activin and Nodal in directing the differentiation of ES cells into genuine DE cells.

Prior to differentiation, wild-type AV3 mouse ES cells (mESCs) were depleted of mouse embryonic fibroblast (MEF) feeders and plated onto gelatin-coated dishes at low density for overnight attachment in mESC medium. The next day, differentiation was induced by switching to reduced serum conditions containing no growth factor (untreated control), or 40, 200 or 1000 ng/ml recombinant Nodal, or 10, 50, 100 or 200 ng/ml recombinant Activin A. Following 7 days of differentiation, expression of the pan-endodermal proteins Sox17 (Kanai-Azuma et al., 2002) and Foxa2 (Ang et al., 1993; Monaghan et al., 1993; Sasaki and Hogan, 1993) was assessed by immunofluorescence and quantification. Consistent with previous reports, we found that both Nodal and Activin induced robust endoderm differentiation, in contrast to untreated controls (supplementary material Fig. S1A). We observed optimal induction of  $79 \pm 6.2\%$  (mean  $\pm$  s.e.m.) Sox17(+) cells with 1000 ng/ml Nodal and  $65.3 \pm 9.8\%$  Sox17(+) cells with 50 ng/ml Activin, compared with  $15.2 \pm 2.8\%$  Sox17(+) cells in controls (supplementary material Fig. S1B). Quantification of cells co-expressing Foxa2 revealed a similar trend across dosage concentrations, with the majority of Sox17(+) cells also expressing Foxa2 (supplementary material Fig. S1A,B). Time-course experiments revealed that peak endoderm output occurred between 6 and 8 days of differentiation with minimal variation in between (data not shown). Therefore, for subsequent studies Nodal and Activin A were used at 1000 ng/ml and 50 ng/ml, respectively, for  $\sim 1$  week.

Next, we characterized the proliferation rate of cells differentiated with Activin A and Nodal across time. mESCs were plated at the same density and the total cell number was compared at 2, 4 and 6 days following endoderm induction. Nodal- and Activin-treated cells appeared similarly healthy during culture and proliferated comparably over the duration of differentiation, even when challenged with different cell-seeding densities and serum concentrations (supplementary material Fig. S1C).

Although *Sox17* and *Foxa2* are required for DE development (Ang et al., 1993; Kanai-Azuma et al., 2002), both genes are also expressed in the extra-embryonic endoderm (ExEn). To date, no unique markers exist for DE, although markers for ExEn are well defined. ExEn cells can therefore be distinguished by their expression of both pan-endoderm and ExEn markers, whereas DE cells can be distinguished by their expression of pan-endoderm markers and lack of ExEn markers. To examine whether Nodal and Activin favor induction of DE or ExEn, we characterized the co-expression of endoderm and ExEn markers using a combination of immunocytochemistry, RT-PCR and quantitative real-time PCR of purified endoderm.

Immunofluorescence analysis showed that neither Nodal- nor Activin-induced endoderm expresses significant levels of the ExEn markers Dab2 (Morrisey et al., 2000), Sparc (Mason et al., 1986), LAMa1 (Lama1 – Mouse Genome Informatics) (Thomas and Dziadek, 1993) and Sox7 (Kanai-Azuma et al., 2002) (supplementary material Fig. S1D). These results contrast with observations in spontaneously differentiated cultures, or cultures treated with retinoic acid (supplementary material Fig. S1D), in which ExEn cells were readily detectable by immunofluorescence and distinct morphology (flattened cells with a high cytoplasmic-to-nuclear ratio). RT-PCR analysis of RNA isolated from ES-derived endoderm also showed that although *Sox17* and *Foxa2* are induced by Nodal and Activin, there is minimal to no expression of the ExEn markers *tPA* (*Plat* – Mouse Genome Informatics) (Strickland et al., 1976), *Hnf4a* (Chen et al., 1994), *Ttr* (Abe et al., 1996), *Amn* (Tomihara-Newberger et al., 1998), *Pem* (*Rhox5* – Mouse Genome Informatics) (Lin et al., 1994), *Lama1* and *Sox7* (supplementary material Fig. S1E).

For quantitative analysis of gene expression, we utilized a Sox17-DsRed mESC line, containing a fluorescent DsRed reporter driven by the *Sox17* promoter (Borowiak et al., 2009). DsRed(+) endodermal cells were purified by flow cytometry following induction by Nodal and Activin. We then harvested RNA from these cells and assessed the expression of additional ExEn markers [*Afp*, *Amn*, *Cldn2*, *Hnf4a*, *Npas2*, *Tcf2* (*Hnf1b* – Mouse Genome Informatics)] (Sherwood et al., 2007) by quantitative RT-PCR. The gene expression profiles of both Nodal- and Activin-derived endoderm more closely resembled DE than ExEn dissected from E8.25 mice (supplementary material Fig. S1F). Together, these results confirm and extend previous findings on Activin (D'Amour et al., 2005; Tada et al., 2005; Yasunaga et al., 2005) to include Nodal, in that both TGF $\beta$  family members preferentially induce DE rather than ExEn *in vitro*, and that this induction occurs with approximately equal effectiveness.

### A functional assay for *in vitro*-derived endoderm

To examine whether ES cell-derived endoderm is functionally equivalent to its embryonic counterpart *in vivo*, we developed a functional assay based on transplantation of ES-derived cells into the mouse embryo for whole embryo *ex vivo* culture. We took advantage of the accessibility of the early embryonic endoderm during gut tube formation (Fig. 1A) (Wells and Melton, 1999). At the completion of gastrulation (E7.5), the embryonic DE comprises a sheet of cells that begins to roll onto itself during gut tube morphogenesis. As rolling initiates, the anterior and posterior ends seal from the outer ends towards the center, forming the anterior and posterior (A/P) intestinal portals (E8.5). Closure of the gut tube, in combination with embryonic turning, results in formation of the primitive gut tube at E9.0. Organ domains then bud and

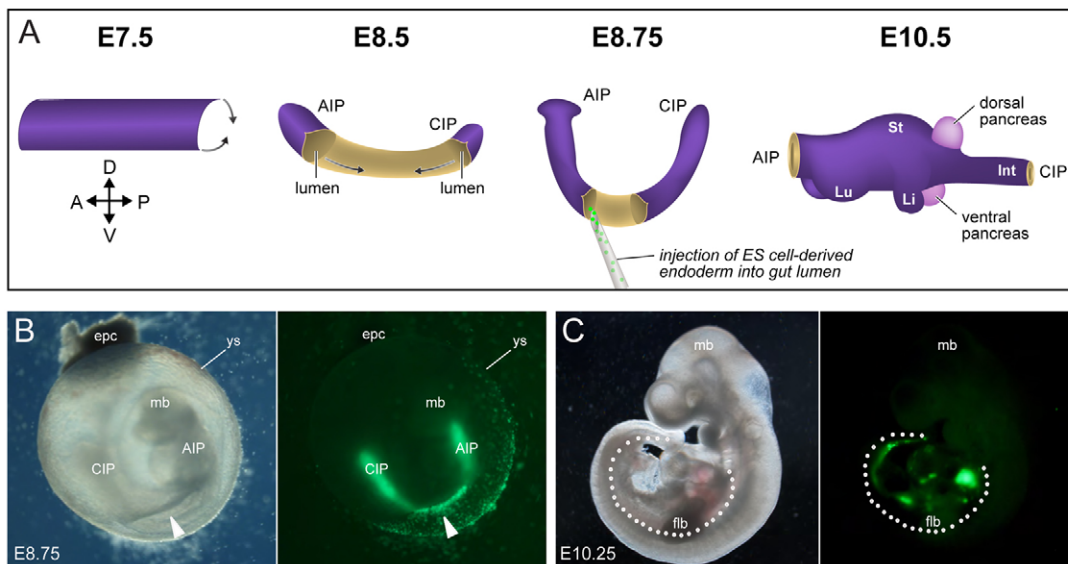


**Fig. 1. A functional assay for ES cell-derived endoderm.** (A) Schematic of DE development in the mouse embryo. ES cell-derived endoderm is injected into the embryonic gut lumen prior to closure (E8.75). (B) Partially turned E8.75 embryo within the yolk sac (ys) following delivery of YFP-labeled ES-derived endoderm into the gut lumen (arrowhead). (C) E10.25 embryo following 24–30 hours of *ex vivo* culture and removal from the yolk sac. Dotted lines indicate embryonic gut tube containing transplanted cells. epc, ectoplacental cone; mb, midbrain; flb, forelimb bud. A, anterior; AIP, anterior intestinal portal; CIP, caudal intestinal portal; D, dorsal; Int, intestine; Li, liver; Lu, lung; P, posterior; St, stomach; V, ventral.

differentiate to form endodermal derivatives, such as the lung, stomach, liver, pancreas and intestine (E10.5).

To address whether *in vitro*-derived endoderm is comparable in identity and function to embryonic endoderm, we deposited ES-derived endoderm into the nascent gut lumen of E8.75 embryos, prior to closure. To track donor ES-derived endoderm cells in host embryos following transplantation, fluorescently labeled mESCs were differentiated with either Nodal or Activin for 7 days, then injected into the developing gut endoderm of unlabeled E8.75 mice (Fig. 1B) for *ex vivo* culture. Embryos were cultured with their yolk sacs intact, as we have found that this aids embryonic development *ex vivo*. Over the course of *ex vivo* culture (24–30 hours), the embryonic gut tube closes, the embryo completes turning, and significant development occurs concomitant with organogenesis (Fig. 1C). Embryos were then harvested at ~E10.25 (supplementary material Movie 1) to assess the fate of injected cells.

### Endoderm generated by Nodal and Activin are functionally distinct *ex vivo*

We began our functional studies by injecting endoderm differentiated from a ubiquitously fluorescent mESC line (Actb-EYFP; Fig. 2A), in which enhanced yellow fluorescent protein is driven by the  $\beta$ -actin promoter (Hadjantonakis et al., 2002). We found that Nodal-induced endoderm contributed to the host gut endoderm with high incidence by efficiently engrafting into the embryonic gut tube in  $57.8 \pm 3.4\%$  of injected embryos ( $n=96$ ; Fig. 2B, top). Furthermore, these cells adopted the morphological characteristics of gut epithelial cells and expressed the gut endoderm markers *Foxa2* and *Cldn6* (Anderson et al., 2008), similar to host endoderm. By contrast, Activin-induced cells contributed to endoderm at a much lower incidence, with only  $11.6 \pm 1.2\%$  of injected embryos exhibiting weak engraftment ( $n=92$ ). The majority of injected cells failed to integrate, and instead remained loosely clustered within the gut lumen along the A/P axis (Fig. 2B, bottom). No improvement was observed in the

engraftment potential of Activin-induced cells even when differentiation was extended to 9–10 days, or upon combined culture with *Wnt3a* (data not shown).

These functional differences were unexpected given the *in vitro* similarity of endoderm gene expression in Nodal- and Activin-induced endoderm (supplementary material Fig. S1). Possible causes for these differences include non-specific effects from either cell culture conditions or the presence of other cell types in the injected population that could contribute to the contrasting phenotypes. For example, if Activin A is intrinsically toxic, cells treated with Activin A might be unhealthy and compromised in function compared with Nodal-differentiated cells. However, this is inconsistent with the observation that Nodal- and Activin-induced endoderm cells show similar growth kinetics (supplementary material Fig. S1C). Alternatively, non-endodermal cell types present in the heterogeneous injected population might hamper the ability of Activin-induced endoderm to interact with endogenous endoderm. We therefore injected purified endoderm following differentiation and cell sorting of a *Sox17*-GFP mESC line (Kim et al., 2007). To track the fate of *Sox17*-GFP-differentiated endoderm following downregulation of *Sox17* during normal maturation of the embryonic gut endoderm, we further labeled these cells by transduction with a lentivirus carrying DsRed under the control of the Ubiquitin promoter (*Sox17*-GFP/Ub-DsRed) (Niakan et al., 2010). Following differentiation with Nodal or Activin A, we selected for GFP-DsRed double-positive cells such that endoderm could be purified (GFP), then tracked long-term (DsRed) after injection into the embryo (Fig. 2C). Injection of purified GFP(+)/DsRed(+) endoderm (Fig. 2D) confirmed previous observations (Fig. 2B). Nodal-derived endoderm readily contributed to the host gut tube, as revealed by epithelialized DsRed-marked cells within the gut tube, which co-expressed *Foxa2* ( $n=8/8$ ; Fig. 2D, top). Despite injection of an equal number of Activin-derived endoderm, these cells still largely failed to contribute to the host gut tube. In the best cases, we observed only

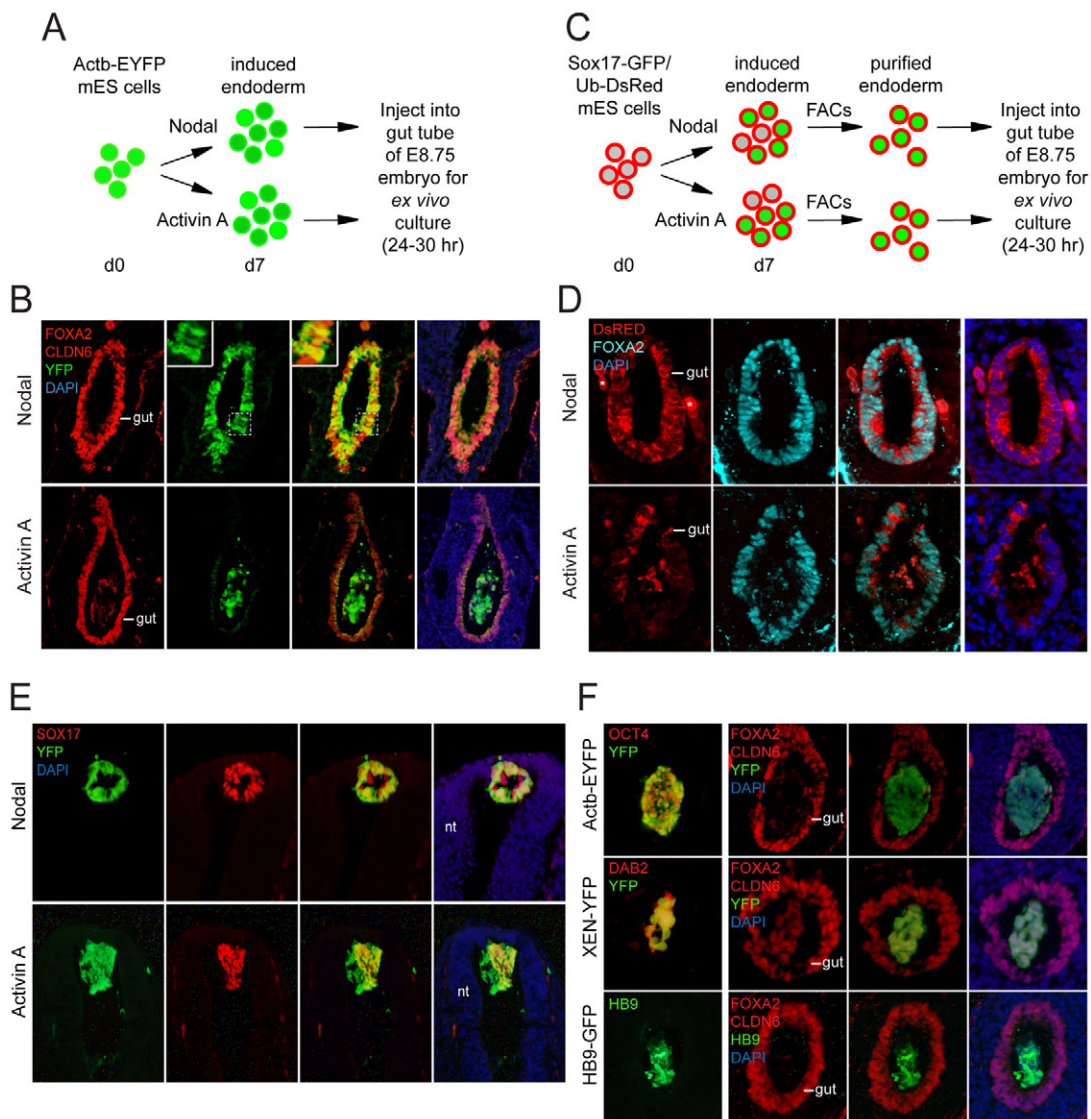


**Fig. 2. Nodal- but not Activin-derived endoderm efficiently contributes to the embryonic endoderm upon transplantation into the mouse embryo.** (A) Differentiation scheme of Actb-EYFP mESCs for functional analysis. d, days of differentiation. (B) Immunofluorescence (IF) analysis of sections of embryos injected with Nodal- or Activin-differentiated Actb-EYFP cells. Foxa2 and Cldn6 mark gut endoderm; YFP marks ES-derived cells, DAPI marks nuclei. Insets: magnified views of engrafted Actb-EYFP endoderm. (C) Differentiation scheme and purification of Sox17-GFP/Ub-DsRed mESCs for functional analysis. (D) IF analysis of sections of embryos injected with purified Nodal- or Activin-differentiated Sox17-GFP(+)/Ub-DsRed(+) cells. (E) IF analysis of sections of embryos in which the neural tube (nt) was injected with Nodal- or Activin-differentiated Actb-EYFP cells. (F) IF analysis of sections of embryos injected with mESCs (Actb-EYFP, Oct4+), ExEn cells (XEN-GFP, Dab2+) or ES-derived motor neurons (HB9-GFP).

a small degree of contribution in both the number of cells per embryo as well in the total number of embryos ( $n=4/18$ ; Fig. 2D, bottom). Figure 2D illustrates the integration of ~40-50 Nodal-derived endodermal cells compared with five to six Activin-derived endodermal cells per plane of section. The majority of Activin-derived endodermal cells were found scattered and unincorporated within the gut lumen. These results exclude indirect effects from non-endodermal cells within the injected population and suggest that Nodal- and Activin-differentiated endoderm differ at a fundamental level in their developmental potential.

As a further functional test, we investigated the tissue specificity of Nodal-derived endoderm with respect to contributions to the host embryo. We injected Nodal-differentiated Actb-EYFP cells

into an alternative luminal structure, the neural tube. In contrast to its behavior when injected into the gut tube, Nodal-induced endoderm does not engraft into the neural tube (Fig. 2E, top), remaining instead as a distinct cluster within the neural lumen. The cells do, however, retain expression of Sox17, suggesting their commitment to the endoderm fate. Interestingly, Nodal-derived Sox17(+) cells often formed independent primitive gut tube-like structures despite residing in ectodermal tissue fated to become brain and spinal cord. Activin-induced endoderm also did not engraft (Fig. 2E, bottom); however, unlike Nodal-induced endoderm, these cells rarely gave rise to organized structures. These results support the contention that contribution of Nodal-derived endoderm to the embryonic gut tube is tissue specific.

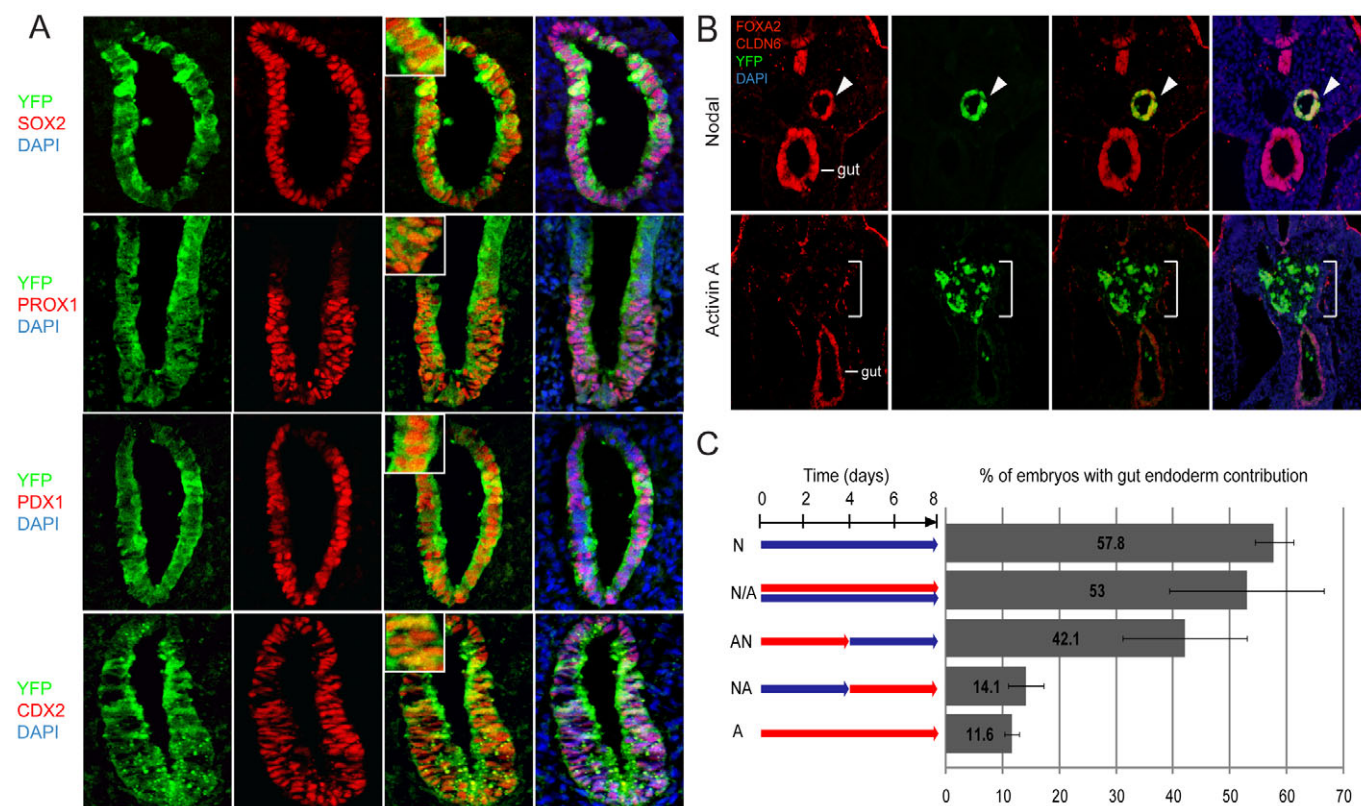


**Fig. 3. Endoderm generated by Nodal and Activin are functionally distinct.** (A) Engrafted Nodal-induced endoderm undergoes organ-specification within the embryonic gut tube. Immunofluorescent (IF) confocal analysis of sections of mouse embryos (1.5  $\mu$ m) following injection of Nodal-differentiated Actb-EYFP into the gut lumen and 30 hours of culture. YFP marks Nodal-induced endoderm; Sox2 marks organs anterior to/including lung; Prox1 marks liver; Pdx1 marks pancreas; Cdx2 marks intestine. Insets: magnification of nuclear marker expression within EYFP(+) donor cells. (B) Nodal- but not Activin-induced endoderm forms ectopic primitive gut tubules. IF analysis of sections of embryos following injection of Actb-EYFP-derived endoderm into the trunk mesenchyme and 24 hours of culture. Arrowheads indicate ectopic gut tubule adjacent to endogenous gut tube; brackets indicate disorganized cells at injection site. Foxa2 and Cldn6 mark endoderm; DAPI marks nuclei. (C) Functional capacity of *in vitro* differentiated endoderm varies based on timing, exposure to Nodal or Activin. Left: outline of mESC exposure (sequentially or in parallel) to Nodal (N) versus Activin (A) over time. Endoderm induction occurred on day zero, cells were injected on d8. Right: percentage of embryos exhibiting gut endoderm contribution following injection of respective endoderm populations. Data represented as mean  $\pm$  s.e.m.

Conversely, to examine whether contribution of donor cells to the gut tube is cell specific, we tested the behavior of other cell types by injecting them into the embryonic gut tube. We used three different kinds of cells: undifferentiated Actb-EYFP cells, ExEn cells derived from mouse blastocysts (XEN) (Kunath et al., 2005), and an alternative ES-derived cell type, motor neurons. Upon injection, all three cell types failed to incorporate into the endogenous endoderm, remaining instead as separate cell clusters within the gut lumen (Fig. 2F). These findings demonstrate that the contribution of donor cells to the gut tube is cell specific and that the ability to efficiently engraft into the host endoderm is specific to Nodal-derived endoderm.

The capability of Nodal-derived endoderm to incorporate into endogenous endoderm (Fig. 2B,D) led us to investigate whether these cells could continue to mature *in vivo* and undergo organ specification. Immunofluorescent confocal analysis of sectioned embryos following extended embryo culture (30 hours) showed that Nodal-differentiated Actb-EYFP cells residing in the gut endoderm appropriately upregulate marker genes for organ domains including the lung (Sox2), liver (Prox1), pancreas (Pdx1) and intestine (Cdx2) (Fig. 3A). Magnified optical sections (1.5  $\mu$ m) confirmed co-expression of these transcription factors in the

nucleus of YFP(+) donor cells (Fig. 3A, insets). Expression of these genes occurred in proper regions along the embryonic axis, with no aberrant expression observed outside the respective organ domains. For example, YFP(+) ES-derived cells only expressed Pdx1 within the A/P regions of the embryo where endogenous Pdx1 could be found, despite engraftment of cells along the length of the embryo. We also note that prior to injection very few cells in the differentiating population expressed Sox2 and Cdx2 (<1-2%), and no cells expressed Pdx1 and Prox1 (data not shown). These data demonstrate that Nodal-derived endoderm can continue development and mature *in vivo*, contributing appropriately to major organ domains along the embryonic A/P axis.

As an additional functional test of ES-derived endoderm, we examined the cell autonomy of Nodal- and Activin-induced Actb-EYFP cells by injecting them into ectopic regions of the embryo, such as the trunk mesenchyme. We found that 66.7% ( $n=48$ ) of embryos injected with Nodal-induced endoderm exhibited formation of ectopic gut tube-like structures (Fig. 3B, top). These tubular structures were positive for both Foxa2 and Cldn6, and measured ~100-150  $\mu$ m in length. By contrast, embryos injected with Activin-induced endoderm exhibited substantially less tubule-forming capacity (7.6%,  $n=46$ ), with cells appearing mainly scattered and

disorganized at the site of injection (Fig. 3B, bottom). These results, together with injections into the neural tube (Fig. 2E), demonstrate that even in non-native environments such as the mesoderm or ectoderm, Nodal-differentiated cells retain their endoderm identity and autonomously organize into primitive gut tubes.

Given the contrasting phenotypes of Nodal- and Activin-induced endoderm, we investigated next whether either factor exerts a dominant effect when applied in sequence or in tandem. We characterized how the exposure and timing of Nodal versus Activin A application would affect the functional capability of the resulting ES-derived endoderm. Sox17-GFP/Ub-DsRed mESCs were treated with Nodal and Activin A serially (Nodal then Activin A, or vice versa) or simultaneously, then sorted for GFP(+)/DsRed(+) endoderm and functionally tested by injection into the embryonic gut tube (Fig. 3C).

When cells were first treated with Nodal (days 0-4), then switched to Activin A for the remainder of differentiation (days 4-8), the percentage of embryos exhibiting gut contribution was similar to those which received fully Activin-differentiated endoderm (days 0-8) (14.1±3.1% versus 11.6±1.2%, respectively). This was a marked difference given that 57.8±3.4% of embryos exhibit gut contribution when injected with fully Nodal-differentiated endoderm (days 0-8), compared with only 14.1±3.1% of embryos when Nodal is replaced with Activin A for the second half of differentiation. Conversely, when cells initially exposed to Activin A (days 0-4) were then switched to Nodal (days 4-8), there was rescue of the Activin A phenotype and cells gained the ability to engraft in the embryonic gut tube at much higher levels (42.1±10.9%). Finally, when Nodal and Activin A were simultaneously applied throughout the duration of differentiation (days 0-8), Nodal effects dominated, and the cells were as capable of contributing to the host gut endoderm as those that were differentiated with Nodal alone (53±13.6% versus 57.8±3.4%, respectively).

These data indicate that Activin A treatment (in part or in full) is insufficient to direct proper differentiation of functionally competent endoderm. Nodal-derived endoderm more closely resembles endogenous endoderm in its ability to identify with and engage in gut tube morphogenesis *in vivo*. More importantly, the observation that Activin-derived endoderm can transition from a functionally incompetent state to a competent state upon additional treatment with Nodal suggests that the two endodermal populations represent related but distinct states of cell potential.

### Gene expression profiling of Nodal- and Activin-derived endoderm

To explore the molecular basis of these functional differences, we purified Nodal- and Activin-derived endoderm and compared their gene expression profiles. Sox17-GFP cells were differentiated in the presence of Nodal or Activin for 7 days, after which GFP(+) cells were purified by FACS. Undifferentiated ES cells were also included for comparison as a control. RNA was isolated from these cells for transcriptional analysis by Illumina microarray profiling (Fig. 4A). Scatter plot analysis showed that both Nodal- and Activin-derived endoderm are distinct from undifferentiated mESCs. The  $r^2$  value (square of linear correlation coefficient) between ES cells and Activin-derived endoderm was 0.8352 (Fig. 4B). Similarly, the  $r^2$  value between ES cells and Nodal-derived endoderm was 0.8495 (Fig. 4C). As expected, undifferentiated ES cells expressed high levels of the pluripotent markers *Oct4* (*Pou5f1* – Mouse Genome Informatics), *Sox2* and *Nanog*, whereas ES-derived endoderm expressed high levels of

endoderm markers, *Sox17*, *Foxa2* and *Cldn6*. When compared against one another, we found that Nodal- and Activin-derived endoderm were highly similar in transcriptional profile (Fig. 4D), with an  $r^2$  value of 0.9937. These results indicate that Nodal- and Activin-derived endoderm are nearly identical in terms of gene expression at the level of global transcription.

Next, we specifically examined the effect of Nodal and Activin on expression levels of genes that typically impact morphogenesis or engraftment, including those involved in cell adhesion, cell attachment and cell migration. No marked differences were observed in the expression of classical cell adhesion factors (cadherins), cell attachment factors (integrins, Icams, Vcam1, Pecam1) or extracellular matrix degrading enzymes that aid in cell migration (matrix metalloproteinases) (Fig. 4E).

Although the two endodermal populations are very similar in global transcription, we questioned whether there might be subtle differences. Among genes differentially expressed at 1.6-fold or greater ( $P \leq 0.05$ ), Nodal-derived endoderm exhibited upregulation of multiple genes involved in either development, maintenance or function of endodermal organs and their cellular derivatives (Fig. 4F). These include *Sst*, *Ghrl*, *Hnf4a*, *Ly64* (*Muc13* – Mouse Genome Informatics), *Ednrb*, *Pcbd* (*Pcbd1* – Mouse Genome Informatics), *Tmprss2*, *Pyy*, *Tbx3*, *Ctsh* and *Pygl*. Activin-derived endoderm lacked upregulation of these genes, instead exhibiting upregulation of key genes expressed in primitive-streak stage embryos, namely, *T* and *Mixl1*. These data suggest that both populations are in the endoderm lineage, sharing expression of *Sox17*, but the molecular identity of the Activin-derived endoderm more closely resembles mesendoderm or nascent endoderm during or shortly after gastrulation, whereas Nodal-derived endoderm more closely resembles endoderm undergoing gut tube morphogenesis and organ-specific differentiation. These results suggest that Nodal- and Activin-derived cells are related in lineage but differ in degree of endoderm progression.

### Nodal- and Activin-derived endoderm differ in pancreatic potential

To explore how ‘poised’ these cells were for downstream differentiation *in vitro*, we examined the developmental competence of ES cell-derived endoderm to undergo subsequent pancreatic specification. Following 6 days of endoderm differentiation with either Nodal or Activin A, culture conditions were switched to promote pancreatic differentiation (Borowiak et al., 2009; Chen et al., 2009; D’Amour et al., 2006). The timing and output of Pdx1, a protein encoded by a gene essential for pancreatic development (Jonsson et al., 1994; Offield et al., 1996), was then analyzed by immunofluorescence and quantified every two days to track the course of pancreatic induction.

Notably, Pdx1 protein expression was detectable earlier in Nodal- versus Activin-induced endoderm (Fig. 5A). Pdx1(+) cells were detected as early as day 8 (2 days following pancreatic induction) in Nodal-treated cells (5.8±1.2%), in contrast to Activin-treated cells (1.4±0.7%), which did not yet exhibit Pdx1 expression levels above untreated controls (1.5±0.7%). On day 10 (4 days following pancreatic induction), Activin-treated cells exhibited more significant levels of Pdx1 induction (6.2±1.3%), although still well below levels observed in Nodal-treated cells (19±3.3%). From this point on, Pdx1 expression continued to increase steadily in both populations, peaking between days 12 and 14, with the overall percentage of Pdx1(+) cells remaining moderately higher in Nodal-treated cells (Nodal: 42.9±1.2%, Activin A: 30.6±6.2%, day 12). Untreated controls exhibited minimal spontaneous activation of

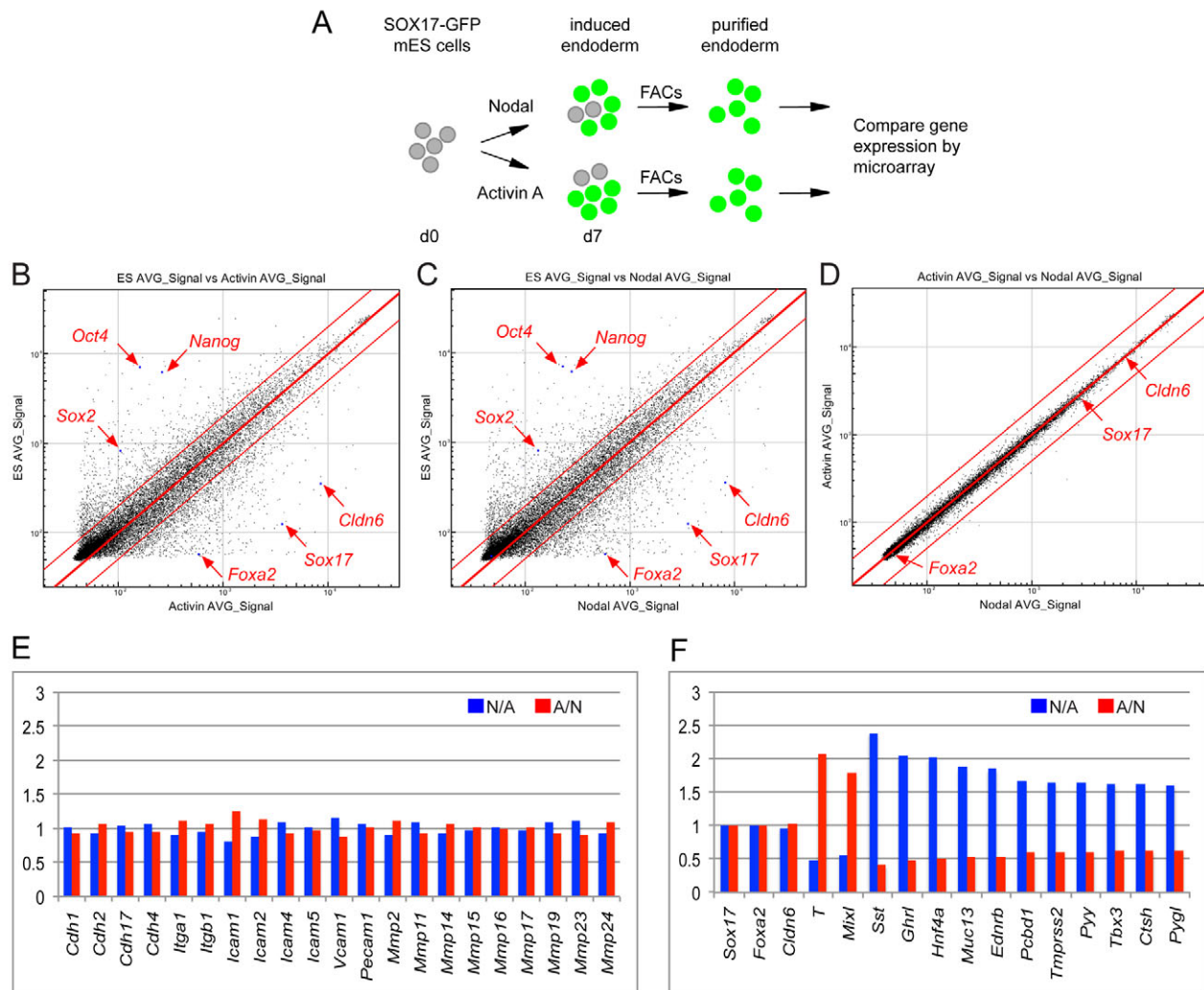


**Fig. 4. Gene expression profiling of Nodal- and Activin-derived endoderm.** (A) Differentiation and purification scheme of Sox17-GFP mouse ES cells for gene expression analysis. (B-D) Scatter plots comparing global gene expression of mESCs versus GFP(+) endoderm from Activin (B) or Nodal (C) treatment, or directly comparing Activin versus Nodal-derived GFP(+) endoderm (D). Center line indicates equivalent levels in gene expression; two flanking lines indicate twofold difference. (E,F) Relative gene expression (y-axis), plotted as ratio of Nodal divided by Activin signal (N/A, blue) or Activin divided by Nodal (A/N, red). (E) Expression of genes involved in cell adhesion [*E-cad* (*Cdh1*), *N-cad* (*Cdh2*), *Cdh17*, *Cdh4*], attachment (*Itga1*, *Itgb1*, *Icam1*, *Icam2*, *Icam4*, *Icam5*, *Vcam1*, *Pcam1*) and migration (*Mmp2*, *Mmp11*, *Mmp14*, *Mmp15*, *Mmp16*, *Mmp17*, *Mmp19*, *Mmp23*, *Mmp24*). (F) Expression of pan endoderm genes (*Sox17*, *Foxa2*, *Cldn6*); primitive streak and mesendoderm genes (*T*, *Mixl*); and genes involved in development, maintenance or function of endodermal organs and their cellular derivatives (*Sst*, *Ghrl*, *Hnf4a*, *Muc13*, *Ednrb*, *Pcbd1*, *Tmprss2*, *Pyy*, *Tbx3*, *Ctsh*, *Pygl*).

Pdx1 expression ( $2.4 \pm 0.2\%$ , day 12). These data suggest that Nodal- and Activin-induced endoderm differ in their propensity to undergo pancreatic differentiation. The temporal delay of Pdx1 induction in Activin- versus Nodal-induced endoderm indicates that the developmental state of the cells is not equal at the onset of pancreatic induction from endoderm. We observed similar differences upon liver differentiation from Activin- versus Nodal-induced endoderm. Nodal-derived endoderm also exhibited greater competency to undergo differentiation into alpha fetoprotein(+) and albumin(+) liver progenitors (supplementary material Fig. S2; data not shown).

Interestingly, we routinely observed two types of Pdx1-expressing cells: those that expressed high levels of Pdx1 (PDX<sup>high</sup>) and those that expressed low levels (PDX<sup>low</sup>). In particular, the majority of pancreatic progenitors derived from

Activin-induced endoderm were PDX<sup>low</sup>, whereas those derived from Nodal-induced endoderm consistently exhibited an increased population of PDX<sup>high</sup> cells (Fig. 5B). Parallel experiments with human ES cell cultures also exhibited the same phenomena of comparable percentage endoderm induction but differential output of Pdx1 expression levels (supplementary material Fig. S3). To characterize the pancreatic progenitor populations generated from Nodal- and Activin-derived endoderm, we quantified PDX<sup>high</sup> and PDX<sup>low</sup> cells by flow cytometry following directed differentiation of a mESC line carrying a GFP reporter under control of the *Pdx1* promoter (Borowiak et al., 2009; Holland et al., 2006). Indeed, PDX<sup>high</sup> and PDX<sup>low</sup> cells were readily detected in both Nodal- and Activin-induced endoderm (day 12; Fig. 5C). However, although the total number of Pdx1(+) cells was comparable, the ratio of PDX<sup>high</sup> to



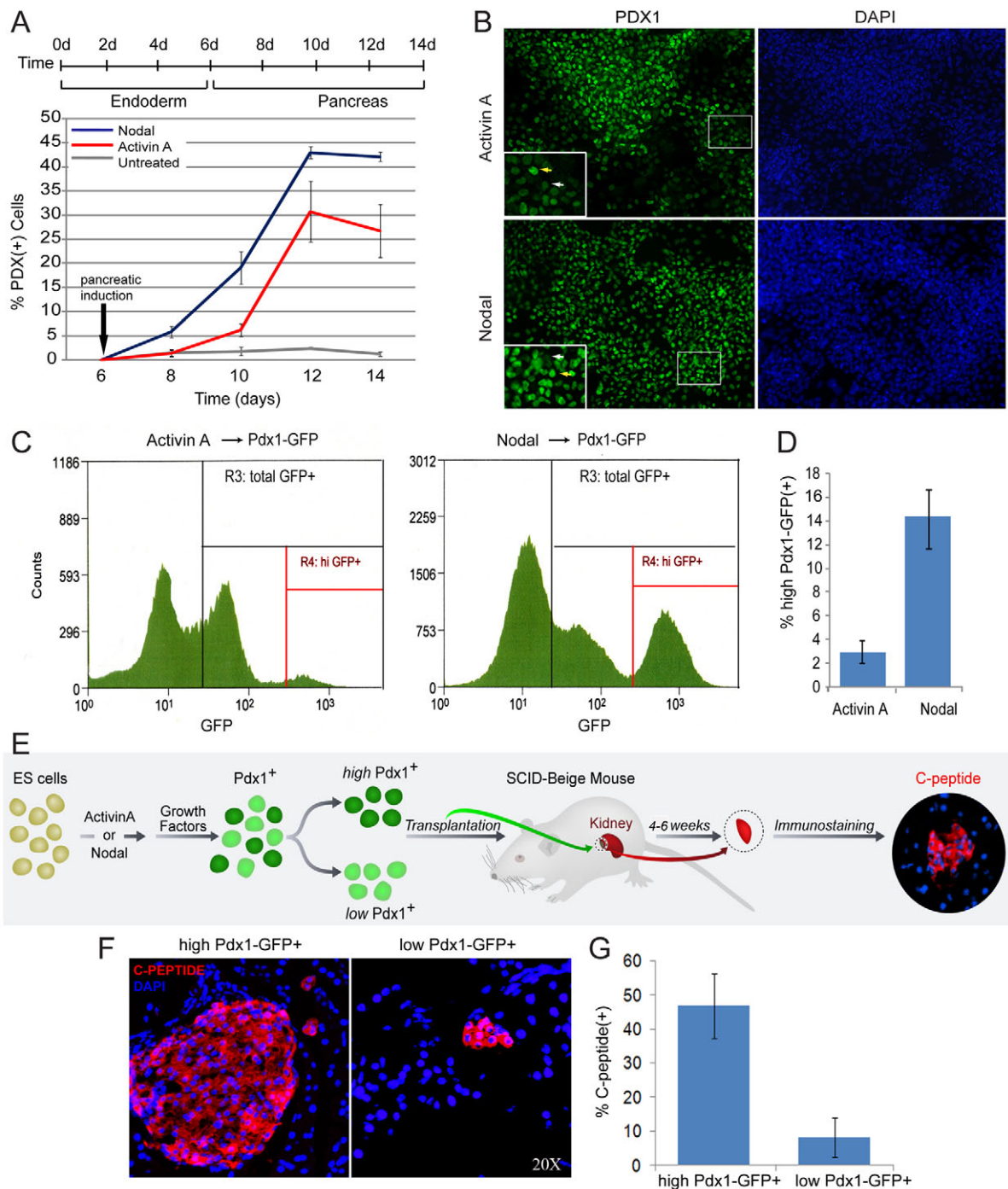


**Fig. 5. Nodal- and Activin-derived endoderm differ in pancreatic potential.** (A) Characterization of Pdx1 induction over time. AV3 mESCs either untreated or treated with Nodal or Activin for 6 days, then differentiated towards pancreatic endoderm. Quantification of Pdx1 expression on days 8, 10, 12 and 14. Data represented as mean±s.e.m. (B) Immunofluorescence (IF) analysis of pancreatic progenitors derived from Nodal- or Activin-induced endoderm. White arrow, PDX<sup>low</sup>; yellow arrow, PDX<sup>high</sup>. Boxed regions are magnified in insets. (C) FACS characterization of pancreatic progenitors derived from Activin- or Nodal-induced Pdx1-GFP mESCs. R3, total GFP(+) cells; R4, GFP<sup>high</sup> cells. (D) Histogram showing quantification of FACS of Pdx1-GFP(+) populations from Activin- and Nodal-induced endoderm. Data represented as mean±s.e.m. (E) Depiction of kidney capsule injection of ES-derived pancreatic endoderm. (F) IF analysis of sections of transplants derived from PDX<sup>high</sup> and PDX<sup>low</sup> injections. C-peptide marks  $\beta$  cells. (G) Quantification of C-peptide(+) cells in grafts 4-6 weeks after transplantation of equal numbers of PDX<sup>high</sup> and PDX<sup>low</sup> cells. Data represented as mean±s.e.m.

PDX<sup>low</sup> cells differed between samples initially exposed to Nodal versus those exposed to Activin A. Specifically, we found that Nodal-induced endoderm led to 14% PDX<sup>high</sup> cells, compared with only 3% PDX<sup>high</sup> for Activin-induced endoderm (Fig. 5D).

To address whether the levels of Pdx1 expression functionally affect or indicate developmental competence, we purified PDX<sup>high</sup> and PDX<sup>low</sup> populations and transplanted them into the kidney capsules of adult mice to assess their potential *in vivo* (Fig. 5E). After

4–6 weeks of incubation in the kidney capsule, the transplants were removed, sectioned and stained for markers of mature pancreatic cells. Particularly, we looked for  $\beta$  cells and the expression of C-peptide. C-peptide(+) cells were detected in transplants derived from both PDX<sup>high</sup> and PDX<sup>low</sup> populations (Fig. 5F). However, transplants derived from injections of PDX<sup>high</sup> cells showed a higher content of  $\beta$  cells, as estimated by the percentage of C-peptide(+) cells per graft: 43% for PDX<sup>high</sup> transplants, in contrast to 9% for PDX<sup>low</sup> (Fig. 5G;  $n=6$  per group). Moreover, in PDX<sup>high</sup> grafts, the C-peptide(+) cells were grouped together as 20- to 50-cell islet-like clusters whereas the PDX<sup>low</sup> the clusters were often scattered, or, at best, arranged in small groups of five to ten cells. We note that, once sorted into PDX<sup>high</sup> and PDX<sup>low</sup> populations, Nodal- and Activin-derived pancreatic progenitors behaved similarly. As endoderm derived from Nodal treatment leads to a greater percentage PDX<sup>high</sup> cells, and PDX<sup>high</sup> cells differentiate more efficiently to C-peptide-expressing cells, these findings together suggest that Nodal signaling is more instructive than Activin A in directing endoderm and pancreatic  $\beta$  cell differentiation *in vitro*.

## DISCUSSION

Directed differentiation of pancreatic  $\beta$  cells from pluripotent stem cells offers tremendous promise for both disease modeling and cell therapy. Although significant progress has been made in the derivation of  $\beta$ -like cells from ES (D'Amour et al., 2006; Jiang et al., 2007; Kroon et al., 2008; Micaleff et al., 2012; Nostro et al., 2011; Zhang et al., 2009) and iPS (Maehr et al., 2009; Park et al., 2008) cells, our understanding of the necessary signals required for the complete derivation of mature  $\beta$  cells *in vitro* is still limited (Naujok et al., 2011). To gain insight into the identity of cells born from *in vitro* differentiation, we evaluated the *in vivo* functional capacity of ES-derived cells at the DE and pancreatic progenitor stages. We present evidence here that, despite exhibiting highly similar transcriptional profiles marked by expression of cardinal endoderm genes, Nodal- and Activin-induced cells are functionally distinct in their potential for endoderm, pancreatic and  $\beta$  cell development.

As a functional assay for endoderm, we transplanted mouse ES-derived endoderm cells into the endoderm compartment of the mouse embryo to test their ability to identify and interact with endogenous endoderm. In contrast to Activin-derived endoderm, Nodal-derived endoderm more efficiently contributes to embryonic gut tube morphogenesis *in vivo*, as well as subsequent differentiation into organ domains, including the lung, liver, pancreas and intestine. Furthermore, Nodal- but not Activin-derived endoderm can autonomously generate primitive gut-tubules upon ectopic injection into mesoderm or ectoderm compartments, such as the trunk mesenchyme and neural tube, respectively. In extended experiments using human ES cell-derived endoderm, we also consistently observed the autonomous formation of tubular structures of 50–75  $\mu\text{m}$  in length by Nodal- but not Activin-differentiated cultures upon injection into the same ectopic sites (supplementary material Fig. S3), suggesting that these differences are conserved between mouse and human ES cells. The finding that two populations of ES-derived endoderm that appear nearly identical *in vitro* behave strikingly differently *in vivo* highlights the notion that the expression of signature genes for a given cell type cannot be assumed to be coupled to functional competency.

Closer examination of gene-profiling results suggested that this functional discrepancy might due to a difference in endoderm progression, with Activin-derived endoderm more closely

resembling mesendoderm or nascent endoderm, whereas Nodal-derived endoderm resembles advanced endoderm poised for gut tube morphogenesis and organ-specific differentiation. Upon continued *in vitro* differentiation towards pancreatic progenitors, we found that Nodal-induced endoderm initiates Pdx1 expression two days earlier than does Activin-induced endoderm, indicating an inherent difference in cellular readiness or ability to respond to pancreatic-inducing cues.

The presence of PDX<sup>high/low</sup> cells indicated that, like pancreatic development in the embryo, pancreatic induction *in vitro* also results in cells expressing variable levels of Pdx1. Here, we found that endoderm derived from Nodal treatment gave rise to 4.6-fold more PDX<sup>high</sup> cells than endoderm derived from Activin A treatment. When PDX<sup>high</sup> and PDX<sup>low</sup> cells were purified and injected into mice, we observed in turn, a sixfold greater efficiency of PDX<sup>high</sup> cells to generate C-peptide(+) cells. These cells were reminiscent of similar populations of PDX<sup>high/low</sup> cells described during mouse pancreatic development *in vivo* (Fujitani et al., 2006; Nelson et al., 2007; Ohlsson et al., 1993). The first Neurog3(+) cells at E10.5 and insulin(+) cells at E12.5 are those expressing high levels of Pdx1, suggesting that the earliest endocrine progenitors and  $\beta$  cells express high levels of Pdx1 (Nelson et al., 2007; Nishimura et al., 2006; Ohlsson et al., 1993). Furthermore, specific depletion of PDX<sup>high</sup> cells by targeted deletion of the *Pdx1* cis-regulatory regions (Area I-II-III) leads to highly defective endocrine development, particularly a failure in  $\beta$ -cell differentiation (Fujitani et al., 2006).

Existing functional assays for pancreatic differentiation interrogate only the final target, the  $\beta$  cell. These read-outs include *in vitro* quantification of insulin release in response to glucose stimulation, as well as *in vivo* rescue of diabetic mouse models upon transplantation of differentiated cells. Despite significant progress in the differentiation of mouse and human ES cells into pancreatic progeny, published protocols have yielded populations of functionally restricted insulin-producing cells akin to immature cells of the fetal pancreas. These cells exhibit a polyhormonal phenotype, lack appropriate glucose responsiveness, or are contaminated with either off-target cell types or ES cells. Here, we present a functional assay that targets the first stage of differentiation into DE. Although it is possible that current protocols sufficiently drive differentiation and maturation to the endocrine but not final  $\beta$  cell stage, our work suggests that functional immaturity already exists at the first stage of endoderm specification in Activin-driven protocols.

Our findings suggest a model in which both Activin and Nodal can generate endoderm and pancreatic cell types *in vitro*, but the efficiency and quality of the resulting cells are not equal. It is possible that endoderm requires maturation prior to organogenesis; perhaps Activin A is able to guide ES cells to an endoderm fate but they remain immature, whereas Nodal can push them further such that they become competent to undergo morphogenesis and organ specification. This is a formal possibility given that Nodal is expressed and required during mouse endoderm development whereas Activin A is not. Although Nodal induces Smad2/3 phosphorylation via the same TypeI/TypeII TGF $\beta$  receptors that Activin A employs, a crucial difference is the obligate presence of the co-receptor Cripto. It therefore remains to be defined whether Cripto confers an additional level of specificity on Smad-dependent signaling and/or conveys Smad-independent effects (Semb, 2008). The findings presented here suggest that Nodal might be the more developmentally relevant molecule for ES cell differentiation into functional endoderm derivatives.

From a global perspective, our observations emphasize the need for more stringent standards in ES cell differentiation and evaluation. Although gene expression analysis is crucial in the initial characterization of ES cell-derived cell types, it is not sufficient. Microarray technology has become highly valuable for identifying complex global changes in gene expression patterns. However, the information obtained by expression profiling is simply the amount of each mRNA species present. Even when we looked beyond the global similarity of Nodal- versus Activin-induced endoderm, we found only a modest difference in a small set of genes, suggestive of a difference in cell states. As cellular processes, including differentiation, are ultimately controlled at the level of the protein, even the same pool of transcripts could lead to variable output of active, properly localized proteins (Lu et al., 2009). All of these factors could result in significant differences in cellular identity and behavior that are not recognizable at the level of the transcriptome and in the absence of rigorous functional assays.

A better understanding of the molecular state of *in vitro*-derived cells is only one of multiple aspects that should be considered when striving for optimal differentiation parameters. In the embryo, pancreas organogenesis a multi-tissue-directed process in which evolving interactions occur between epithelia, mesenchyme and endothelial cells. It is therefore likely that generation of fully differentiated  $\beta$  cells will require co-culture with pancreatic mesenchyme (Sneddon et al., 2012), endothelial cells, or their purified derivatives. Three-dimensional culture environments may also facilitate this process and ultimately aid in the development, maturation and function of *in vitro*-differentiated  $\beta$  cells. Together, these strategies will provide a grounded basis for continued progress in the derivation of insulin-producing cells for disease research and regenerative biology.

#### Acknowledgements

We thank C. Wright for goat anti-Pdx1 antibody; S. Morrison for Sox17-GFP mESCs; A. Nagy and K. Hadjantonakis for YFP-labeled mESCs; J. Dimos for providing Ub-DsRed lentivirus; and K. Niakan for generating Ub-DsRed labeled Sox17-GFP mESCs. HB9-GFP mES-derived motor neurons were kindly provided by G. Boulting. We also thank P. Rogers and B. Tilton for FACS support; and R. Helmiss for illustrative support. We thank Q. Zhou, J. Rajagopal and K. Niakan for experimental advice and manuscript review.

#### Funding

A.E.C. is a fellow of the Jane Coffin Childs Memorial Fund for Medical Research. M.B. was supported by the Beta Cell Biology Consortium and the Leona M. and Harry B. Helmsley Charitable Trust. D.A.M. is an Investigator of the Howard Hughes Medical Institute. Deposited in PMC for release after 6 months.

#### Competing interests statement

The authors declare no competing financial interests.

#### Supplementary material

Supplementary material available online at <http://dev.biologists.org/lookup/suppl/doi:10.1242/dev.085431/-/DC1>

#### References

- Abe, K., Niwa, H., Iwase, K., Takiguchi, M., Mori, M., Abé, S. I., Abe, K. and Yamamura, K. I. (1996). Endoderm-specific gene expression in embryonic stem cells differentiated to embryoid bodies. *Exp. Cell Res.* **229**, 27-34.
- Agarwal, S., Holton, K. and Lanza, R. (2008). Efficient differentiation of functional hepatocytes from human embryonic stem cells. *Stem Cells* **26**, 1117-1127.
- Anderson, W. J., Zhou, Q., Alcalde, V., Kaneko, O. F., Blank, L. J., Sherwood, R. I., Guseh, J. S., Rajagopal, J. and Melton, D. A. (2008). Genetic targeting of the endoderm with claudin-6CreER. *Dev. Dyn.* **237**, 504-512.
- Ang, S. L., Wierda, A., Wong, D., Stevens, K. A., Cascio, S., Rossant, J. and Zaret, K. S. (1993). The formation and maintenance of the definitive endoderm lineage in the mouse: involvement of HNF3/forkhead proteins. *Development* **119**, 1301-1315.
- Bach, J. F. (1994). Insulin-dependent diabetes mellitus as an autoimmune disease. *Endocr. Rev.* **15**, 516-542.
- Basford, C. L., Prentice, K. J., Hardy, A. B., Sarangi, F., Micallef, S. J., Li, X., Guo, Q., Elefanty, A. G., Stanley, E. G., Keller, G. et al. (2012). The functional and molecular characterisation of human embryonic stem cell-derived insulin-positive cells compared with adult pancreatic beta cells. *Diabetologia* **55**, 358-371.
- Blyszczuk, P., Czyz, J., Kania, G., Wagner, M., Roll, U., St-Onge, L. and Wobus, A. M. (2003). Expression of Pax4 in embryonic stem cells promotes differentiation of nestin-positive progenitor and insulin-producing cells. *Proc. Natl. Acad. Sci. USA* **100**, 998-1003.
- Borowiak, M., Maehr, R., Chen, S., Chen, A. E., Tang, W., Fox, J. L., Schreiber, S. L. and Melton, D. A. (2009). Small molecules efficiently direct endodermal differentiation of mouse and human embryonic stem cells. *Cell Stem Cell* **4**, 348-358.
- Chen, W. S., Manova, K., Weinstein, D. C., Duncan, S. A., Plump, A. S., Prezioso, V. R., Bachvarova, R. F. and Darnell, J. E., Jr (1994). Disruption of the HNF-4 gene, expressed in visceral endoderm, leads to cell death in embryonic ectoderm and impaired gastrulation of mouse embryos. *Genes Dev.* **8**, 2466-2477.
- Chen, S., Borowiak, M., Fox, J. L., Maehr, R., Osafune, K., Davidow, L., Lam, K., Peng, L. F., Schreiber, S. L., Rubin, L. L. et al. (2009). A small molecule that directs differentiation of human ESCs into the pancreatic lineage. *Nat. Chem. Biol.* **5**, 258-265.
- D'Amour, K. A., Agulnick, A. D., Eliazar, S., Kelly, O. G., Kroon, E. and Baetge, E. E. (2005). Efficient differentiation of human embryonic stem cells to definitive endoderm. *Nat. Biotechnol.* **23**, 1534-1541.
- D'Amour, K. A., Bang, A. G., Eliazar, S., Kelly, O. G., Agulnick, A. D., Smart, N. G., Moorman, M. A., Kroon, E., Carpenter, M. K. and Baetge, E. E. (2006). Production of pancreatic hormone-expressing endocrine cells from human embryonic stem cells. *Nat. Biotechnol.* **24**, 1392-1401.
- Ding, J., Yang, L., Yan, Y. T., Chen, A., Desai, N., Wynshaw-Boris, A. and Shen, M. M. (1998). Cripto is required for correct orientation of the anterior-posterior axis in the mouse embryo. *Nature* **395**, 702-707.
- Fujitani, Y., Fujitani, S., Boyer, D. F., Gannon, M., Kawaguchi, Y., Ray, M., Shiota, M., Stein, R. W., Magnuson, M. A. and Wright, C. V. (2006). Targeted deletion of a cis-regulatory region reveals differential gene dosage requirements for Pdx1 in foregut organ differentiation and pancreas formation. *Genes Dev.* **20**, 253-266.
- Gadue, P., Huber, T. L., Paddison, P. J. and Keller, G. M. (2006). Wnt and TGF- $\beta$  signaling are required for the induction of an *in vitro* model of primitive streak formation using embryonic stem cells. *Proc. Natl. Acad. Sci. USA* **103**, 16806-16811.
- Gouon-Evans, V., Boussemaert, L., Gadue, P., Nierhoff, D., Koehler C., Kubo, A., Shafritz, D. and Keller, G. (2006). BMP-4 is required for hepatic specification of mouse embryonic stem cell-derived definitive endoderm. *Nat. Biotechnol.* **24**, 1402-1411.
- Grapin-Botton, A. and Constam, D. (2007). Evolution of the mechanisms and molecular control of endoderm formation. *Mech. Dev.* **124**, 253-278.
- Hadjantonakis, A. K., Macmaster, S. and Nagy, A. (2002). Embryonic stem cells and mice expressing different GFP variants for multiple non-invasive reporter usage within a single animal. *BMC Biotechnol.* **2**, 11.
- Hansson, M., Tonning, A., Frandsen, U., Petri, A., Rajagopal, J., Englund, M. C., Heller, R. S., Håkansson, J., Fleckner, J., Sköld, H. N. et al. (2004). Artfactual insulin release from differentiated embryonic stem cells. *Diabetes* **53**, 2603-2609.
- Hansson, M., Olesen, D. R., Peterslund, J. M., Engberg, N., Kahn, M., Winzig, M., Klein, T., Maddox-Hyttel, P. and Serup, P. (2009). A late requirement for Wnt and FGF signaling during activin-induced formation of foregut endoderm from mouse embryonic stem cells. *Dev. Biol.* **330**, 286-304.
- Holland, A. M., Micallef, S. J., Li, X., Elefanty, A. G. and Stanley, E. G. (2006). A mouse carrying the green fluorescent protein gene targeted to the Pdx1 locus facilitates the study of pancreas development and function. *Genesis* **44**, 304-307.
- Hori, Y., Rulifson, I. C., Tsai, B. C., Heit, J. J., Cahoy, J. D. and Kim, S. K. (2002). Growth inhibitors promote differentiation of insulin-producing tissue from embryonic stem cells. *Proc. Natl. Acad. Sci. USA* **99**, 16105-16110.
- Jiang, W., Shi, Y., Zhao, D., Chen, S., Yong, J., Zhang, J., Qing, T., Sun, X., Zhang, P., Ding, M. et al. (2007). *In vitro* derivation of functional insulin-producing cells from human embryonic stem cells. *Cell Res.* **17**, 333-344.
- Jonsson, J., Carlsson, L., Edlund, T. and Edlund, H. (1994). Insulin-promoter factor 1 is required for pancreas development in mice. *Nature* **371**, 606-609.
- Kanai-Azuma, M., Kanai, Y., Gad, J. M., Tajima, Y., Taya, C., Kurohmaru, M., Sanai, Y., Yonekawa, H., Yazaki, K., Tam, P. P. et al. (2002). Depletion of definitive gut endoderm in Sox17-null mutant mice. *Development* **129**, 2367-2379.

- Kim, I., Saunders, T. L. and Morrison, S. J. (2007). Sox17 dependence distinguishes the transcriptional regulation of fetal from adult hematopoietic stem cells. *Cell* **130**, 470-483.
- Kroon, E., Martinson, L. A., Kadoya, K., Bang, A. G., Kelly, O. G., Eliazar, S., Young, H., Richardson, M., Smart, N. G., Cunningham, J. et al. (2008). Pancreatic endoderm derived from human embryonic stem cells generates glucose-responsive insulin-secreting cells in vivo. *Nat. Biotechnol.* **26**, 443-452.
- Kubo, A., Shinozaki, K., Shannon, J. M., Kouskoff, V., Kennedy, M., Woo, S., Fehling, H. J. and Keller, G. (2004). Development of definitive endoderm from embryonic stem cells in culture. *Development* **131**, 1651-1662.
- Kunath, T., Arnaud, D., Uy, G. D., Okamoto, I., Chureau, C., Yamanaka, Y., Heard, E., Gardner, R. L., Avner, P. and Rossant, J. (2005). Imprinted X-inactivation in extra-embryonic endoderm cell lines from mouse blastocysts. *Development* **132**, 1649-1661.
- Lewis, S. L. and Tam, P. P. (2006). Definitive endoderm of the mouse embryo: formation, cell fates, and morphogenetic function. *Dev. Dyn.* **235**, 2315-2329.
- Lin, T. P., Labosky, P. A., Grabel, L. B., Kozak, C. A., Pitman, J. L., Kleeman, J. and MacLeod, C. L. (1994). The *Pem* homeobox gene is X-linked and exclusively expressed in extraembryonic tissues during early murine development. *Dev. Biol.* **166**, 170-179.
- Lowe, L. A., Yamada, S. and Kuehn, M. R. (2001). Genetic dissection of nodal function in patterning the mouse embryo. *Development* **128**, 1831-1843.
- Lu, R., Markowitz, F., Unwin, R. D., Leek, J. T., Airoidi, E. M., MacArthur, B. D., Lachmann, A., Rozov, R., Ma'ayan, A., Boyer, L. A. et al. (2009). Systems-level dynamic analyses of fate change in murine embryonic stem cells. *Nature* **462**, 358-362.
- Lumelsky, N., Blondel, O., Laeng, P., Velasco, I., Ravin, R. and McKay, R. (2001). Differentiation of embryonic stem cells to insulin-secreting structures similar to pancreatic islets. *Science* **292**, 1389-1394.
- Maehr, R., Chen, S., Snitow, M., Ludwig, T., Yagasaki, L., Goland, R., Leibel, R. L. and Melton, D. A. (2009). Generation of pluripotent stem cells from patients with type 1 diabetes. *Proc. Natl. Acad. Sci. USA* **106**, 15768-15773.
- Mason, I. J., Taylor, A., Williams, J. G., Sage, H. and Hogan, B. L. (1986). Evidence from molecular cloning that SPARC, a major product of mouse embryonic parietal endoderm, is related to an endothelial cell 'culture shock' glycoprotein of *M*, 43,000. *EMBO J.* **5**, 1465-1472.
- Micallef, S. J., Janes, M. E., Knezevic, K., Davis, R. P., Elefanty, A. G. and Stanley, E. G. (2005). Retinoic acid induces Pdx1-positive endoderm in differentiating mouse embryonic stem cells. *Diabetes* **54**, 301-305.
- Micallef, S. J., Li, X., Schiesser, J. V., Hirst, C. E., Yu, Q. C., Lim, S. M., Nostro, M. C., Elliott, D. A., Sarangi, F., Harrison, L. C. et al. (2012). *INS<sup>(GFP<sup>β</sup>)</sup>* human embryonic stem cells facilitate isolation of *in vitro* derived insulin-producing cells. *Diabetologia* **55**, 694-706.
- Monaghan, A. P., Kaestner, K. H., Grau, E. and Schütz, G. (1993). Postimplantation expression patterns indicate a role for the mouse forkhead/HNF-3 alpha, beta and gamma genes in determination of the definitive endoderm, chordamesoderm and neuroectoderm. *Development* **119**, 567-578.
- Morrisey, E. E., Musco, S., Chen, M. Y., Lu, M. M., Leiden, J. M. and Parmacek, M. S. (2000). The gene encoding the mitogen-responsive phosphoprotein Dab2 is differentially regulated by GATA-6 and GATA-4 in the visceral endoderm. *J. Biol. Chem.* **275**, 19949-19954.
- Naujok, O., Burns, C., Jones, P. M. and Lenzen, S. (2011). Insulin-producing surrogate  $\beta$ -cells from embryonic stem cells: are we there yet? *Mol. Ther.* **19**, 1759-1768.
- Nelson, S. B., Schaffer, A. E. and Sander, M. (2007). The transcription factors Nkx6.1 and Nkx6.2 possess equivalent activities in promoting beta-cell fate specification in Pdx1+ pancreatic progenitor cells. *Development* **134**, 2491-2500.
- Niakan, K. K., Ji, H., Maehr, R., Vokes, S. A., Rodolfa, K. T., Sherwood, R. I., Yamaki, M., Dimos, J. T., Chen, A. E., Melton, D. A. et al. (2010). Sox17 promotes differentiation in mouse embryonic stem cells by directly regulating extraembryonic gene expression and indirectly antagonizing self-renewal. *Genes Dev.* **24**, 312-326.
- Nishimura, W., Kondo, T., Salameh, T., El Khattabi, I., Dodge, R., Bonner-Weir, S. and Sharma, A. (2006). A switch from MafB to MafA expression accompanies differentiation to pancreatic beta-cells. *Dev. Biol.* **293**, 526-539.
- Nostro, M. C., Sarangi, F., Ogawa, S., Holtzinger, A., Corneo, B., Li, X., Micallef, S. J., Park, I. H., Basford, C., Wheeler, M. B. et al. (2011). Stage-specific signaling through TGF family members and WNT regulates patterning and pancreatic specification of human pluripotent stem cells. *Development* **138**, 861-871.
- Offield, M. F., Jetton, T. L., Labosky, P. A., Ray, M., Stein, R. W., Magnuson, M. A., Hogan, B. L. and Wright, C. V. (1996). PDX-1 is required for pancreatic outgrowth and differentiation of the rostral duodenum. *Development* **122**, 983-995.
- Ohlsson, H., Karlsson, K. and Edlund, T. (1993). IPF1, a homeodomain-containing transactivator of the insulin gene. *EMBO J.* **12**, 4251-4259.
- Park, I. H., Arora, N., Huo, H., Maherali, N., Ahfeldt, T., Shimamura, A., Lensch, M. W., Cowan, C., Hochedlinger, K. and Daley, G. Q. (2008). Disease-specific induced pluripotent stem cells. *Cell* **134**, 877-886.
- Raikwar, S. P. and Zavazava, N. (2009). Insulin producing cells derived from embryonic stem cells: are we there yet? *J. Cell. Physiol.* **218**, 256-263.
- Rajagopal, J., Anderson, W. J., Kume, S., Martinez, O. I. and Melton, D. A. (2003). Insulin staining of ES cell progeny from insulin uptake. *Science* **299**, 363.
- Rezania, A., Riedel, M. J., Wideman, R. D., Karanu, F., Ao, Z., Warnock, G. L. and Kieffer, T. J. (2011). Production of functional glucagon-secreting  $\alpha$ -cells from human embryonic stem cells. *Diabetes* **60**, 239-247.
- Sasaki, H. and Hogan, B. L. (1993). Differential expression of multiple fork head related genes during gastrulation and axial pattern formation in the mouse embryo. *Development* **118**, 47-59.
- Schier, A. F. (2003). Nodal signaling in vertebrate development. *Annu. Rev. Cell Dev. Biol.* **19**, 589-621.
- Semb, H. (2008). Definitive endoderm: a key step in coaxing human embryonic stem cells into transplantable beta-cells. *Biochem. Soc. Trans.* **36**, 272-275.
- Sherwood, R. I., Jitianu, C., Cleaver, O., Shaywitz, D. A., Lamenzo, J. O., Chen, A. E., Golub, T. R. and Melton, D. A. (2007). Prospective isolation and global gene expression analysis of definitive and visceral endoderm. *Dev. Biol.* **304**, 541-555.
- Sneddon, J., Borowiak, M. and Melton, D. (2012). Self-renewal of embryonic-stem-cell-derived progenitors by organ-matched mesenchyme. *Nature* **491**, 765-768.
- Soria, B., Roche, E., Berná, G., León-Quinto, T., Reig, J. A. and Martín, F. (2000). Insulin-secreting cells derived from embryonic stem cells normalize glycemia in streptozotocin-induced diabetic mice. *Diabetes* **49**, 157-162.
- Stainier, D. Y. (2002). A glimpse into the molecular entrails of endoderm formation. *Genes Dev.* **16**, 893-907.
- Strickland, S., Reich, E. and Sherman, M. I. (1976). Plasminogen activator in early embryogenesis: enzyme production by trophoblast and parietal endoderm. *Cell* **9**, 231-240.
- Tada, S., Era, T., Furusawa, C., Sakurai, H., Nishikawa, S., Kinoshita, M., Nakao, K., Chiba, T. and Nishikawa, S. (2005). Characterization of mesendoderm: a diverging point of the definitive endoderm and mesoderm in embryonic stem cell differentiation culture. *Development* **132**, 4363-4374.
- Tam, P. P., Kanai-Azuma, M. and Kanai, Y. (2003). Early endoderm development in vertebrates: lineage differentiation and morphogenetic function. *Curr. Opin. Genet. Dev.* **13**, 393-400.
- Thomas, T. and Dziadek, M. (1993). Expression of laminin and nidogen genes during the postimplantation development of the mouse placenta. *Biol. Reprod.* **49**, 1251-1259.
- Tian, T. and Meng, A. M. (2006). Nodal signals pattern vertebrate embryos. *Cell. Mol. Life Sci.* **63**, 672-685.
- Tomihara-Newberger, C., Haub, O., Lee, H. G., Soares, V., Manova, K. and Lacy, E. (1998). The *amn* gene product is required in extraembryonic tissues for the generation of middle primitive streak derivatives. *Dev. Biol.* **204**, 34-54.
- Vincent, S. D., Dunn, N. R., Hayashi, S., Norris, D. P. and Robertson, E. J. (2003). Cell fate decisions within the mouse organizer are governed by graded Nodal signals. *Genes Dev.* **17**, 1646-1662.
- Wells, J. M. and Melton, D. A. (1999). Vertebrate endoderm development. *Annu. Rev. Cell Dev. Biol.* **15**, 393-410.
- Yasunaga, M., Tada, S., Torikai-Nishikawa, S., Nakano, Y., Okada, M., Jakt, L. M., Nishikawa, S., Chiba, T., Era, T. and Nishikawa, S. (2005). Induction and monitoring of definitive and visceral endoderm differentiation of mouse ES cells. *Nat. Biotechnol.* **23**, 1542-1550.
- Zhang, D., Jiang, W., Liu, M., Sui, X., Yin, X., Chen, S., Shi, Y. and Deng, H. (2009). Highly efficient differentiation of human ES cells and iPS cells into mature pancreatic insulin-producing cells. *Cell Res.* **19**, 429-438.
- Zhou, Q. and Melton, D. A. (2008). Pathways to new beta cells. *Cold Spring Harb. Symp. Quant. Biol.* **73**, 175-181.
- Zorn, A. M. and Wells, J. M. (2007). Molecular basis of vertebrate endoderm development. *Int. Rev. Cytol.* **259**, 49-111.